IEEE Access
Multidisciplinary | Rapid Review | Open Access Journal

Received July 26, 2019, accepted August 26, 2019, date of publication September 2, 2019, date of current version September 26, 2019.

Digital Object Identifier 10.1109/ACCESS.2019.2938999

Control of Z-Axis MEMS Gyroscope Using Adaptive Fractional Order Dynamic Sliding Mode Approach

HUIMIN WANG[1], LIANG HUA[1], YUNXIANG GUO[1], AND CHENG LU[1,2]
[1]School of Electrical Engineering, Nantong University, Nantong 226019, China
[2]Nantong Research Institute for Advanced Communication Technologies, Nantong 226000, China

Corresponding author: Cheng Lu (garcia_lu@126.com)

This work was supported in part by the Foundation of Nantong Research Institute for Advanced Communication Technologies under Grant KFKT2017A01, in part by the Nantong University-Nantong Joint Research Center for Intelligent Information Technology under Grant KFKT2017A01, in part by the Natural Science Key Research Program of Jiangsu Colleges under Grant 17KJA470006, and in part by the National Natural Science Foundation of China under Grant 61673226 and Grant 51877112.

ABSTRACT This paper proposes a states feedback control method for Z-axis MEMS gyroscopes using fractional calculus and adaptive dynamic sliding mode control method. A new sliding mode control method is proposed to achieve trajectory tracking by adding a fractional order term in the conventional sliding manifold. The new proposed sliding surface contains integer order terms as well as fractional order terms and thus can provide an extra degree of freedom. Besides, in the presence of unknown system parameters, some adaptive laws containing the new designed sliding manifold are proposed to online tune controller parameters. All adaptive laws are derived in the stability framework and the stability of the control system is also guaranteed according to the Lyapunov stability theory and. Simulations results on a Z-axis vibrating gyroscope are provided to illustrate the effectiveness of the control method.

INDEX TERMS Adaptive control, dynamic sliding mode control, gyroscope, fractional order calculus.

I. INTRODUCTION

MEMS gyroscopes are commonly used sensors for measuring angular velocity which are widely used in many occasions such as cell phone, navigation, quadcopter and so on. The working principle of MEMS gyroscopes is based on the inertia effect of the detecting mass caused by the Colioris force. Due to the defect of manufacturing technology, the structure of the MEMS gyroscope is not totally symmetric, and the asymmetric will cause quadrature coupling between the driving axis and the sensing axis. Besides, there are also parameter variation and external disturbance in the gyroscope system. All the above-mentioned factors will deteriorate the performance of the MEMS gyroscope. To address these problems, great efforts have been dedicated in the investigation of MEMS gyroscope control methods. Various control methods including sliding mode control, adaptive control and other techniques are all applied in the control of MEMS gyroscopes [1]–[3].

The associate editor coordinating the review of this manuscript and approving it for publication was Xudong Zhao.

Sliding mode control (SMC) is a powerful robust control scheme which has been widely used in many areas [4]–[6]. SMC has many attractive features such as easy implementation, insensitive to parameter variation, robust to disturbance and so on and these advantages make SMC a useful tool in the control of system dynamics. SMC has many advantages while it also has its drawbacks. It can be found from the structure of sliding mode control that there are always discontinuous robust terms in the control force. The discontinuous terms will cause chattering in control forces and the high frequency chattering will damage actuators in practical situations. How to achieve satisfactory control performance while reducing chattering phenomenon is always a hot topic since SMC was firstly introduced [4]. Dynamic sliding mode control method is one kind of high order sliding mode control method that can alleviate chattering problem by transferring discontinuous term to the derivative of the control force [7]–[10]. As a consequence, dynamic sliding mode control technique has attracted increasing attention and it is widely used in many occasions. Hwang *et al.* [7] proposed a hierarchically improved fuzzy dynamic sliding mode control method in the control of autonomous ground

vehicle to achieve path tracking. In [8], Liu developed a new dynamic terminal sliding manifold and applied the new dynamic sliding control method in the control of a class of SISO systems. Utkin discussed to what extent the high order sliding mode control may serve as an alternative to the conventional sliding mode control in [9]. In [10], Fridman proposed a continuous super twisting control which is based on higher order sliding mode observer and the control method can achieve second-order sliding mode.

Adaptive control is an effective approach to handle parameter variations and it is usually combined with many other control methods to improve performances of control systems [11]–[16] in the presence of unknown parameters [17]–[20]. Banazadeh and Taymourtash [14] proposed an adaptive control method for an insect-like flapping wing air vehicle where adaptive control technique is combined with sliding mode control for attitude and position control. A novel direct adaptive tracking control scheme is established in [16] by incorporating fuzzy systems to approximate nonlinear functions.

Fractional calculus is a generalization and extension of integer differentiation and integration to fractional orders. As a branch of mathematics, this concept has attracted increasing attention of scientists and researchers due to its importance in the investigation of system modeling and control algorithms. Fractional calculus has also been integrated with adaptive control techniques [21]–[23] for system performances improvement. Fei and Lu [21] proposed an adaptive fractional order sliding mode control method for a Z-axis gyroscope where a neural network is used to alleviate chattering. In [22], Ahmad and Hamidreza analyzed dynamics of chaotic fractional order systems under adaptive sliding mode control method. In [23], Ali and Hamed proposed a new fractional order dynamic sliding mode method for a class of nonlinear systems.

Thus, fractional calculus can also be used in adaptive dynamic sliding mode control (ADSMC) for MEMS gyroscopes. Gyroscope performances and parameter adaptation performances under adaptive fractional order dynamic sliding mode control (AFDSMC) shall be systematically investigated as well. At the same time, the effects on control performances and parameter adaptations performances caused by different fractional orders shall also be studied in detail. To the best of our known, control methods for MEMS gyroscopes using fractional order dynamic sliding mode control method are seldom explored in the literature.

This paper proposed a dynamic sliding mode control method using fractional calculus and simulation is conducted on a Z-axis gyroscope to validate the effectiveness of the control scheme. The main contribution of the paper can be concluded as follows:

(1) One superior characteristic of the proposed control scheme is that the control method developed conventional sliding method by adding a fractional order term in the sliding manifold which can provide an extra degree of freedom, so that one can achieve better trajectory tracking performance as well as parameter adaptation performance compared to conventional integer order sliding mode method. This is the most important feature of the proposed method, as compared with conventional gyroscope control methods.

(2) The proposed control method improves system tracking performance as well as robustness by dealing with system nonlinearities such as parameter variation and external disturbances. Then adaptive fractional order dynamic sliding mode control methods has been extended to the control of MEMS gyroscopes. This is a successful example using fractional calculus and dynamic sliding mode control with the MEMS gyroscope.

(3) Adaptive laws are proposed in the stability framework to online tune system parameters and the stability of the entire control system is guaranteed using Lyapunov stability theorem. It shall be mentioned that all the adaptive algorithms contain fractional order terms which can provide more flexibility in the controller design as well as parameters adaptation process. Besides, as long as persistent excitation condition [11] is satisfied, all system parameters can be correctly estimated.

The rest of the paper is organized as follows: in section 2, an introduction of fractional calculus is presented and a MEMS gyroscope system model is given. In section 3, an adaptive fractional order dynamic sliding mode controller is studied and the stability of the control system is also provided. Section 4 shows the simulation results and section 5 gives the conclusions.

II. PRELIMINARY AND SYSTEM DESCRIPTION

Factional calculus is a generalization of integration and differentiation to fractional order fundamental operation [24], [25]. Denoted by ${}_aD_t^\alpha$, the fractional order operator takes both fractional order derivative and fractional integral in a single expression defined as:

$$ {}_aD_t^\alpha = \begin{cases} \dfrac{d^\alpha}{dt^\alpha} & \alpha > 0 \\ 1 & \alpha = 0 \\ \displaystyle\int_a^t (d\tau)^{-\alpha} & \alpha < 0 \end{cases} \tag{1} $$

where a and t are the limits of the operator and α is the fractional order of the operator. There are three most commonly used definitions for general fractional order operator.

Definition 1: for $n-1 < \alpha < n \in Z^+$, the $\alpha - th$ order Grunwald-Letnikov(GL) fractional derivative [24], [25] is expressed as

$$ {}_aD_t^\alpha f(t) = \lim_{h\to 0} h^{-\alpha} \sum_{j=0}^{[(t-a)/h]} (-1)^j \binom{\alpha}{j} f(t-jh) \tag{2} $$

where $[(t-a)/h]$ represents the max integer number which is less than $(t-a)/h$, $\binom{\alpha}{j} = \frac{\Gamma(\alpha+1)}{\Gamma(k+1)\Gamma(n-k+1)}$ and $\Gamma(\bullet)$ is the gamma function, $\Gamma(\gamma) = \int_0^\infty e^{-t}t^{\gamma-1}dt$.

Definition 2: The $\alpha - th$ order Riemann-Letnikov(RL) fractional derivative [24], [25] is written as

$$D^\alpha f(t) = \frac{d^n}{dt^n}[\frac{1}{\Gamma(n-\alpha)}\int_0^t \frac{f(\tau)}{(t-\tau)^{\alpha-n+1}}d\tau] \tag{3}$$

where $n-1 < \alpha < n \in Z^+$.

Definition 3: The $\alpha - th$ order Caputo fractional derivative [24], [25] is defined as

$$D^\alpha f(t) = \frac{1}{\Gamma(n-\alpha)}\int_0^t \frac{f(\tau)}{(t-\tau)^{\alpha-n+1}}d\tau \tag{4}$$

where $n-1 < \alpha < n \in Z^+$.

In the following parts, we will use Caputo definition in the control method design and the operator is denoted by D^α for clarity [26], [27].

Generally speaking, a typical Z-axis vibratory gyroscope contains a proof mass, spring beams, electrostatic actuators and sensing mechanisms. In the gyroscope, the proof mass can only move in the X-O-Y plane and the gyroscope is rotating at a constant angular velocity around the Z-axis. Due to limitation of manufacturing technology, the gyroscope structure is not totally symmetric which will cause extra coupling between X and Y axis. The motion equation [13] of the gyroscope is derived as:

$$\begin{cases} m\ddot{x} + d_{xx}\dot{x} + d_{xy}\dot{y} + k_{xx}x + k_{xy}y = u_x + 2m\Omega_z\dot{y} \\ m\ddot{y} + d_{xy}\dot{x} + d_{yy}\dot{y} + k_{xy}x + k_{yy}y = u_y - 2m\Omega_z\dot{x} \end{cases} \tag{5}$$

where m is the weight of the proof mass; x and y are the coordinates of the mass; k_{xx} k_{yy} d_{xx} d_{yy} are the spring coefficients and damping coefficients in the X and Y direction; d_{xy} k_{xy} are the extra coupling terms caused by the asymmetric structure and friction imperfection; Ω_z is the angular velocity and $u_x u_y$ represent control forces in the X and Y direction.

Dividing both sides of (5) by the reference mass m, the reference length q_0 and the resonance frequency ω_0^2, we can get the motion equation in non-dimensional form as

$$\begin{cases} \ddot{x}^* + d_{xx}^*\dot{x}^* + d_{xy}^*\dot{y}^* + \omega_x^2 x^* + \omega_{xy}y^* = u_x^* + 2\Omega_z^*\dot{y}^* \\ \ddot{y}^* + d_{xy}^*\dot{x}^* + d_{yy}^*\dot{y}^* + \omega_{xy}x^* + \omega_y^2 y^* = u_y^* - 2\Omega_z^*\dot{x}^* \end{cases} \tag{6}$$

where$x^* = \frac{x}{q_0}$, $y^* = \frac{y}{q_0}$, $\dot{x}^* = \frac{x}{q_0\omega_0}$, $\dot{y}^* = \frac{y}{q_0\omega_0}$, $\ddot{x}^* = \frac{\ddot{x}}{q_0\omega_0^2}$, $\ddot{y}^* = \frac{\ddot{y}}{q_0\omega_0^2}$, $d_{xx}^* = \frac{d_{xx}}{m\omega_0}$, $d_{xy}^* = \frac{d_{xy}}{m\omega_0}$, $d_{yy}^* = \frac{d_{yy}}{m\omega_0}$, $\Omega_z^* = \frac{\Omega_z}{\omega_0}$, $\omega_x = \sqrt{\frac{k_{xx}}{m\omega_0^2}}$, $\omega_y = \sqrt{\frac{k_{yy}}{m\omega_0^2}}$, $\omega_{xy} = \frac{k_{xy}}{m\omega_0^2}$, $u_x^* = \frac{u_x}{mq_0\omega_0^2}$, $u_y^* = \frac{u_y}{mq_0\omega_0^2}$.

Rewriting (6) in vector form yields

$$\ddot{q} + D\dot{q} + Kq = u - 2\Omega\dot{q} \tag{7}$$

where

$$q = \begin{bmatrix} x^* \\ y^* \end{bmatrix}, \quad u = \begin{bmatrix} u_x^* \\ u_y^* \end{bmatrix}, \quad D = \begin{bmatrix} d_{xx}^* & d_{xy}^* \\ d_{xy}^* & d_{yy}^* \end{bmatrix},$$
$$K = \begin{bmatrix} \omega_x^2 & \omega_{xy} \\ \omega_{xy} & \omega_y^2 \end{bmatrix}, \quad \Omega = \begin{bmatrix} 0 & -\Omega_z^* \\ \Omega_z^* & 0 \end{bmatrix}.$$

Taking parameters variation and external disturbances into consideration, we can further get the motion equation in vector form as

$$\begin{aligned} \ddot{q} &= u - (D + 2\Omega)\dot{q} - Kq - (\Delta D + 2\Delta\Omega)\dot{q} - \Delta Kq + d \\ &= u - (D + 2\Omega)\dot{q} - Kq + F \end{aligned} \tag{8}$$

For simplicity, (8) is rewritten in the form

$$\ddot{q} = f + u + F \tag{9}$$

where $f = -(D + 2\Omega)\dot{q} - Kq$, q is the state vector, u is the control vector and $F = \begin{bmatrix} F_1 \\ F_2 \end{bmatrix}$ represents lumped, matched unknown disturbances including parameters variation and external disturbance, expressed as $F = -(\Delta D + 2\Delta\Omega)\dot{q} - \Delta Kq + d$.

Assumption 1: The lumped parameter uncertainties and external disturbance F is bounded such that $|F_i| \le F_{di}$ $i = 1, 2$. The derivative of the lumped parameter uncertainties and external disturbance is bounded such that $|\dot{F}_i| \le \dot{F}_{di}$ $i = 1, 2$, where $F_{di}, \dot{F}_{di}$ $i = 1, 2$ are positive constants.

In the next section, an adaptive fraction order dynamic manifold is proposed and the design of an adaptive fractional order dynamic sliding mode controller is investigated so that gyroscope trajectory can track the reference trajectory.

III. ADAPTIVE FRACTIONAL ORDER DYNAMIC SLIDING MODE CONTROLLER

A. DESIGN OF FRACTIONAL ORDER DYNAMIC SLIDING MODE CONTROL

An adaptive fractional order dynamic sliding mode controller is established with the objective to find a control law so that the gyroscope state q can track a reference trajectory q_d. Assuming that all parameters in the gyroscope system are well known, the design of an ideal fractional dynamic sliding mode controller is described step by step as follows:

Define the tracking error as

$$e = q_d - q \tag{10}$$

The derivative of tracking error is

$$\dot{e} = \dot{q}_d - \dot{q} \tag{11}$$

Define a fractional order sliding surface as

$$S = \dot{e} + c_2 e + c_3 D^{\alpha-1} e \tag{12}$$

where $c_2 = \begin{bmatrix} c_{21} & 0 \\ 0 & c_{22} \end{bmatrix}$, $c_3 = \begin{bmatrix} c_{31} & 0 \\ 0 & c_{32} \end{bmatrix}$ are sliding surface parameters which are chosen to be diagonal matrixes with the diagonal elements c_{2i}, c_{3i}, $i = 1, 2$ being positive constants. $\alpha - 1$ is the fractional order of fractional order operation.

The derivative of the sliding surface is

$$\begin{aligned}\dot{S} &= \ddot{e} + c_2\dot{e} + c_3 D^{\alpha} e \\ &= (\ddot{q}_d - \ddot{q}) + c_2(\dot{q}_d - \dot{q}) + c_3 D^{\alpha} e \\ &= (\ddot{q}_d + (D + 2\Omega)\dot{q} + Kq - u) \\ &\quad + c_2(\dot{q}_d - \dot{q}) + c_3 D^{\alpha} e \end{aligned} \tag{13}$$

A fractional order dynamic sliding manifold is designed as

$$\begin{aligned}\sigma &= \dot{S} + \partial S \\ &= \ddot{e} + c_2\dot{e} + c_3 D^{\alpha} e + (\dot{e} + c_2 e + c_3 D^{\alpha-1} e) \end{aligned} \tag{14}$$

where $\partial = \begin{bmatrix} \partial_1 & 0 \\ 0 & \partial_2 \end{bmatrix}$ is the dynamic sliding surface parameter where $\partial_i,\ i = 1, 2$ are positive constants.

It can be seen from the definition of the dynamic sliding manifold in (14) that if $\sigma \to 0$, $\dot{S} + \partial S = 0$ is a stable system only if all the roots of $\dot{S} + \partial S = 0$ are located in the left half plane. That is to say if $\sigma \to 0$, the sliding surface designed in (12) will converge to zero with ∂ being a positive diagonal matrix. And it can be inferred from the definition of the sliding surface in (12) that the tracking error will also converge to zero.

Differentiating both sides of (4), the derivative of the dynamic surface is

$$\begin{aligned}\dot{\sigma} &= \ddot{S} + \partial\dot{S} \\ &= \dddot{e} + c_2\ddot{e} + c_3 D^{\alpha+1} e + \partial(\ddot{e} + c_2\dot{e} + c_3 D^{\alpha} e) \\ &= \dddot{e} + (c_2 + \partial)\ddot{e} + c_3 D^{\alpha+1} e + \partial c_3 D^{\alpha} e + \partial c_2\dot{e} \\ &= (\dddot{q}_d - \dddot{q}) + (c_2 + \partial)(\ddot{q}_d - \ddot{q}) \\ &\quad + c_3 D^{\alpha+1} e + \partial c_3 D^{\alpha} e + \partial c_2\dot{e} \\ &= (\dddot{q}_d - \dot{f} - \dot{u} - \dot{F}) + (c_2 + \partial)(\ddot{q}_d - f - u - F) \\ &\quad + c_3 D^{\alpha+1} e + \partial c_3 D^{\alpha} e + \partial c_2\dot{e} \end{aligned} \tag{15}$$

Then, a sliding mode controller can be designed in the following form

$$u = u_{eq} + u_{sw} \tag{16}$$

where

$$\begin{aligned} u_{eq} &= (c_2 + \partial)^{-1}[(\dddot{q}_d - \dot{f} - \dot{u}_{eq}) \\ &\quad + (c_2 + \partial)(\ddot{q}_d - f - \dot{u}_{eq}) \\ &\quad + c_3 D^{\alpha+1} e + \partial c_3 D^{\alpha} e + \partial c_2\dot{e}] \end{aligned} \tag{17}$$

$$u_{sw} = (c_2 + \partial)^{-1}\eta sgn(\sigma) \tag{18}$$

$\eta = \begin{bmatrix} \eta_1 & 0 \\ 0 & \eta_2 \end{bmatrix}$ is the robust gain of the switch term and $\eta_i,\ i = 1, 2$ chosen to be positive constants.

Theorem 1: If the control force designed in (16) is applied to the MEMS gyroscope system described in (9), the entire control system is stable.

Proof: Choose a Lyapunov candidate as

$$V = \frac{1}{2}\sigma^T\sigma \tag{19}$$

Differentiating both sides of (19) and substituting (15) into $\dot{V}$ leads to

$$\begin{aligned}\dot{V} &= \sigma^T\dot{\sigma} \\ &= \sigma^T[(\dddot{q}_d - \dot{f} - \dot{u} - \dot{F}) \\ &\quad + (c_2 + \partial)(\ddot{q}_d - f - u - F) \\ &\quad + c_3 D^{\alpha+1} e + \partial c_3 D^{\alpha} e + \partial c_2\dot{e}] \end{aligned} \tag{20}$$

Substituting the control force in (16) into (20) yields

$$\begin{aligned}\dot{V} &= \sigma^T\dot{\sigma} \\ &= \sigma^T(-\eta sgn(\sigma)) \\ &= -\eta\left|\sigma^T\right| \le 0 \end{aligned} \tag{21}$$

Since the Lyapunov function is positive definite and the derivative of the Lyapunov function is negative definite, according to the Lyapunov stability theorem, it can be concluded that the entire control system is asymptotically stable.

B. DESIGN OF ADAPTIVE FRACTIONAL ORDER DYNAMIC SLIDING MODE CONTROL

If the system parameters are unknown, the dynamic sliding mode controller designed in (16) cannot be implemented directly. Adaptive control technique is adopted in this part to online tune the unknown system parameters in (16).

Control force in (16) can be modified in the new form

$$\begin{aligned}\hat{u}_{eq} &= (c_2 + \partial)^{-1}[(q_d - \dot{\hat{f}} - \dot{u}_{eq}) \\ &\quad + (c_2 + \partial)(\ddot{q}_d - \hat{f} - \dot{\hat{u}}_{eq}) \\ &\quad + c_3 D^{\alpha+1} e + \partial c_3 D^{\alpha} e + \partial c_2\dot{e}] \end{aligned} \tag{22}$$

where $\hat{f} = -(\hat{D} + 2\hat{\Omega})\dot{q} - \hat{K}q$ is an estimate of f.

And the proposed modified adaptive controller is designed as

$$\hat{u} = \hat{u}_{eq} + u_{sw} \tag{23}$$

where $\hat{u}_{eq}$ is shown in (22) and u_{sw} remains the same as (18).

In order to update the system parameters in (23), the adaptive laws are given in the following form

$$\dot{\hat{D}}^T = \eta_1\ddot{q}\sigma^T + \eta_1\dot{q}\sigma^T(c_2 + \partial) \tag{24}$$

$$\dot{\hat{\Omega}}^T = 2(\eta_3\ddot{q}\sigma^T + \eta_3\dot{q}\sigma^T(c_2 + \partial)) \tag{25}$$

$$\dot{\hat{K}}^T = \eta_2\dot{q}\sigma^T + \eta_2 q\sigma^T(c_2 + \partial) \tag{26}$$

The block diagram of the designed adaptive fractional order sliding mode control system is depicted in Fig.1.

Theorem 2: If the designed controller in (23) and the adaptive laws in (24), (25), (26) are applied to the system in (9), the entire control system is asymptotically stable, system tracking errors will converge to zero and all the system parameters can be correctly estimated.

Proof: Choose a new Lyapunov candidate as

$$\begin{aligned} V &= \frac{1}{2}\sigma^T\sigma + \frac{1}{2}tr(\tilde{D}^T\frac{1}{\eta_1}\tilde{D}) \\ &\quad + \frac{1}{2}tr(\tilde{K}^T\frac{1}{\eta_2}\tilde{K}) + \frac{1}{2}tr(\tilde{\Omega}^T\frac{1}{\eta_3}\tilde{\Omega}) \end{aligned} \tag{27}$$

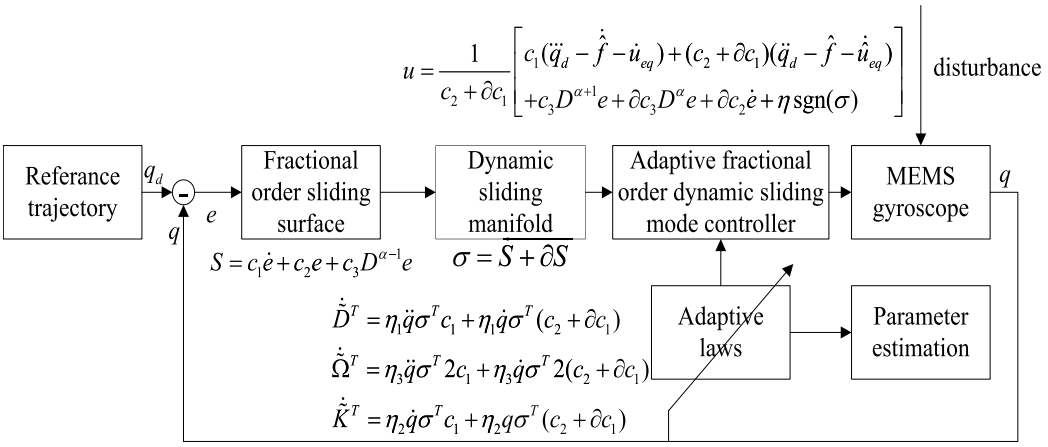

FIGURE 1. Block diagram of the adaptive dynamic sliding mode controller.

where σ is the dynamic sliding manifold, $\tilde{D}$, $\tilde{K}$, $\tilde{\Omega}$ are the estimation errors of the known system parameters defined such that $D - \hat{D} = -\tilde{D}$, $\Omega - \hat{\Omega} = -\tilde{\Omega}$, $K - \hat{K} = -\tilde{K}$.

Differentiating both sides of (27) and substituting (15) into $\dot{V}$ yield

$$\begin{aligned}\dot{V} &= \sigma^T\dot{\sigma} + tr(\dot{\tilde{D}}^T\frac{1}{\eta_1}\tilde{D}) + tr(\dot{\tilde{K}}^T\frac{1}{\eta_2}\tilde{K}) + tr(\dot{\tilde{\Omega}}^T\frac{1}{\eta_3}\tilde{\Omega}) \\ &= \sigma^T\begin{bmatrix}(\dddot{q}_d - \ddot{f} - \dot{u}) + (c_2+\partial)(\ddot{q}_d - f - u) \\ +c_3 D^{\alpha+1}e + \partial c_3 D^{\alpha}e + \partial c_2\dot{e}\end{bmatrix} + tr(*)\end{aligned} \tag{28}$$

where $tr(\dot{\tilde{D}}^T\frac{1}{\eta_1}\tilde{D}) + tr(\dot{\tilde{K}}^T\frac{1}{\eta_2}\tilde{K}) + tr(\dot{\tilde{\Omega}}^T\frac{1}{\eta_3}\tilde{\Omega})$ is denoted as $tr(*)$ for clarity.

Substituting the adaptive controller in (23) into (28) gives

$$\begin{aligned}\dot{V} &= \sigma^T\begin{bmatrix}(\dddot{q}_d - \ddot{f} - \dot{u} - \dot{F}) + (c_2+\partial)(\ddot{q}_d - f - u - F) \\ +c_3 D^{\alpha+1}e + \partial c_3 D^{\alpha}e + \partial c_2\dot{e}\end{bmatrix} \\ &\quad + tr(*) \\ &= \sigma^T[\dddot{q}_d - \ddot{f} - \dot{u} - \dot{F} + (c_2+\partial)\ddot{q}_d - (c_2+\partial)f \\ &\quad -(c_2+\partial)(c_2+\partial)^{-1}((\dddot{q}_d - \dot{\hat{f}} - \dot{u}) \\ &\quad + (c_2+\partial)(\ddot{q}_d - \hat{f} - \hat{u}) - (c_2+\partial)F \\ &\quad + c_3 D^{\alpha+1}e + \partial c_3 D^{\alpha}e + \partial c_2\dot{e} + \eta sgn(\sigma)) \\ &\quad + c_3 D^{\alpha+1}e + \partial c_3 D^{\alpha}e + \partial c_2\dot{e}] + tr(*) \\ &= \sigma^T[-\dot{F} - (c_2+\partial)F - \ddot{f} + \dot{\hat{f}} - (c_2+\partial)f \\ &\quad + (c_2+\partial)\hat{f} - \eta sgn(\sigma)] + tr(*) \\ &= \sigma^T[-\dot{F} - (c_2+\partial)F + \dot{\tilde{f}} + (c_2+\partial)\tilde{f} \\ &\quad - \eta sgn(\sigma)] + tr(*)\end{aligned} \tag{29}$$

where $\tilde{f} = \hat{f} - f$ and $\tilde{f}$ is described as

$$\begin{aligned}\tilde{f} &= -(\hat{D} + 2\hat{\Omega})\dot{q} - \hat{K}q - (-(D+2\Omega)\dot{q} - Kq) \\ &= [(D-\hat{D}) + 2(\Omega - \hat{\Omega})]\dot{q} + (K - \hat{K})q \\ &= (-\tilde{D} - 2\tilde{\Omega})\dot{q} - \tilde{K}q\end{aligned} \tag{30}$$

The derivative of $\tilde{f}$ is given in the form

$$\dot{\tilde{f}} = (-\tilde{D} - 2\tilde{\Omega})\ddot{q} - \tilde{K}\dot{q} \tag{31}$$

Substituting (31) into (29) yields

$$\begin{aligned}\dot{V} &= \sigma^T[-\dot{F} - (c_2+\partial)F] \\ &\quad + \sigma^T\{[(-\tilde{D} - 2\tilde{\Omega})\ddot{q} - \tilde{K}\dot{q}] \\ &\quad + (c_2+\partial)[(-\tilde{D} - 2\tilde{\Omega})\dot{q} - \tilde{K}q] - \eta sgn(\sigma)\} \\ &\quad + tr(*) \\ &= \sigma^T[-\dot{F} - (c_2+\partial)F] \\ &\quad + \sigma^T\{[-\tilde{D}\ddot{q} - (c_2+\partial)\tilde{D}\dot{q}] \\ &\quad + [-2\tilde{\Omega}\ddot{q} - 2(c_2+\partial)\tilde{\Omega}\dot{q}] \\ &\quad + [-\tilde{K}\dot{q} - (c_2+\partial)\tilde{K}q] - \eta sgn(\sigma)\} \\ &\quad + tr(*) \\ &= \sigma^T[-\dot{F} - (c_2+\partial)F] \\ &\quad + [-\ddot{q}\sigma^T\tilde{D} - \dot{q}\sigma^T(c_2+\partial)\tilde{D}] + tr(\frac{\dot{\tilde{D}}^T\tilde{D}}{\eta_1}) \\ &\quad + [-2\ddot{q}\sigma^T\tilde{\Omega} - 2\dot{q}\sigma^T(c_2+\partial)\tilde{\Omega}] + tr(\frac{\dot{\tilde{\Omega}}^T\tilde{\Omega}}{\eta_3}) \\ &\quad + [-\dot{q}\sigma^T\tilde{K} - q\sigma^T(c_2+\partial)\tilde{K}] + tr(\frac{\dot{\tilde{K}}^T\tilde{K}}{\eta_2}) - \eta|\sigma|\end{aligned} \tag{32}$$

Substituting adaptive laws in (24), (25), (26) into (32) yields

$$\dot{V} = \sigma^T[-\dot{F} - (c_2+\partial)F] - \eta\left|\sigma^T\right| \tag{33}$$

With **Assumption 1**, we can further get

$$\dot{V} \le [\dot{F}_d + (c_2+\partial)F_d - \eta]\left|\sigma^T\right| \tag{34}$$

If the robust sliding gain η is selected so that $\eta \ge [\dot{F}_d + (c_2+\partial)F_d]$, $\dot{V} \le 0$. $\dot{V}$ is semi-negative definite implies that $\sigma, \tilde{D}, \tilde{K}, \tilde{\Omega}$ are all bounded. It can be concluded from (15) that $\dot{\sigma}$ is also bounded. The inequality $\dot{V} \le [\dot{F}_d + (c_2+\partial)F_d - \eta]\left|\sigma^T\right|$ implies that σ^T is integrable as $\int_0^t \left|\sigma^T\right|dt \le \frac{1}{\dot{F}_d + (c_2+\partial)F_d - \eta}(V(0) - V(t))$. Since $V(0)$ is bounded, $V(t)$ is bounded and non-increasing. It can be

concluded that $\int_0^t |\sigma^T|dt$ is also bounded. Since $\int_0^t |\sigma^T|dt$ is bounded and $\dot{\sigma}$ is also bounded, according to Barbalart lemma, σ will asymptotically converge to zero, $\lim_{t\to\infty} \sigma = 0$. It can be concluded from (12) and (14) that e will asymptotically converge to zero. The sliding surface and tracking error will converge to zero asymptotically;

For the adaptive laws (24), (25) and (26), according to the theory of persistence excitation [11], if the reference trajectory $q_d = \begin{bmatrix} x_d \\ y_d \end{bmatrix} = \begin{bmatrix} A_1 \sin(\omega_1 t) \\ A_2 \sin(\omega_2 t) \end{bmatrix}$ is persistence excitation signals, i.e., $\omega_1 \neq \omega_2$, $\tilde{D}, \tilde{K}, \tilde{\Omega}$ will converge to zero, D, K, Ω will converge to their true values. All the parameters can be estimated correctly.

Remark: It can be found that the robust gain shall meet the condition that $\eta \geq [\dot{F}_d + (c_2 + \partial)F_d]$. The condition may lead to a very big robust gain, but if controller parameters c_2, ∂ are chosen to be very small, the robust gain can be arbitrary small.

IV. SIMULATION STUDY

This section has 3 parts, where trajectory tracking performances using ADSMC and AFDSMC are presented and parameters adaptation performances are also shown in the first part. In the second part, system responses under AFDSMC with different fractional orders are provided. Parameter adaptation performances under different fractional orders are also shown in the second part. In the third part, system dynamics with frequency deviation are studied.

It shall be emphasized that all the parameters in the design of sliding surfaces, dynamic surfaces, and adaptive laws are all the same. The only difference between ADSMC and AFDSMC is that a fractional term is added in the design of AFDSMC controller while the sliding surface of ADSMC has only integral terms. And in the second part, all simulation results are derived using AFDSMC with exactly the same parameters; the only difference is that the fractional orders are different.

As an illustrative example, we use a z-axis gyroscope dynamic model [13] for the study of adaptive fractional order dynamic sliding mode controller.

Parameters of the gyroscope dynamic model (7) are set as follows:

$$\begin{aligned} m &= 1.8 \times 10^{-7} kg, \quad k_{xx} = 63.955 N/m, \\ k_{yy} &= 95.92 N/m, \quad k_{xy} = 12.779 N/m, \\ d_{xx} &= 1.8 \times 10^{-6} N \bullet s/m, \quad d_{yy} = 1.8 \times 10^{-6} N \bullet s/m, \\ d_{xy} &= 3.6 \times 10^{-7} N \bullet s/m. \end{aligned}$$

Choose a reference length $q_0 = 1\mu m$, reference frequency $\omega_0 = 1kHz$, and the angular velocity $\Omega_z = 100 rad/s$. The parameters can be obtained through non-dimensional transformation $\omega_x^2 = 355.3$, $\omega_y^2 = 532.9$, $\omega_{xy} = 70.99$, $d_{xx}^* = 0.01$, $d_{yy}^* = 0.01$, $d_{xy}^* = 0.002$, $\Omega_z^* = 0.1$.

Initial conditions on matrix D, K, Ω are $D(0) = 0.95D$, $K(0) = 0.95K$, $\Omega(0) = 0.95\Omega$. The desired motion trajectory

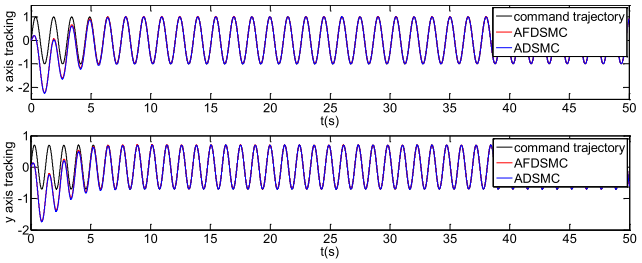

FIGURE 2. Comparison of tracking performances using ADSMC and AFDSMC.

$x_d = \sin(4.11t)$ to $x_d = \sin(2.085t)$ and $y_d = 0.7\sin(5.11t)$ to $y_d = 0.7\sin(2.555t)$ at time point $t = 12\pi/4.17$ in X axis and $t = 12\pi/5.11$ in Y axis. External disturbances are $d = \begin{bmatrix} d_1 \\ d_2 \end{bmatrix} = \begin{bmatrix} rand(1) \\ rand(1) \end{bmatrix}$ where disturbance in each channel is uniformly distributed between 0-1.

Parameters of ADSMC and AFDSMC and Gains of adaptive laws (24)-(26) are provided in Table.1.

A. COMPARISONS BETWEEN ADSMC AND AFDSMC

System trajectory tracking performances and tracking errors using ADSMC and AFDSMC are shown in Fig.2 and Fig.3. It can be found from Fig.2 that both red line (AFDSMC) and blue line (ADSMC) can track the black line (command trajectory) in a few seconds and the three lines almost overlap with each other in the end. In is shown in Fig.3 that both blue line (ADSMC) and red line (AFDSMC) will converge to zero, this means that system tracking errors using ADSMC and AFDSMC will converge to zero. It can be observed from the partial enlarged pictures in both tracking error figures that red lines (AFDSMC) response more quickly than blue lines (ADSMC) and red lines (AFDSMC) use less time than blue line (ADSMC) to converge to zero, this means that the fractional order terms in AFDSMC scheme can improve system transient performances.

Fig.4 and Fig.5 depict adaptation performances of system parameters and angular velocity. It can be clearly seen from Fig.4 that red line (AFDSMC) uses less time to become stable and the values red and blue lines converge to are exactly system parameters we set in the system. It can be seen in Fig.5 that both blue line (ADSMC) and red line (AFDSMC) are going up and down around 0.1 which is just the angular velocity set in the system. That is to say the adaptive laws using fractional order terms can correctly estimate system parameters and fractional order adaptive laws has better parameter identification performance than integral order adaptive laws.

Fig.6 depicts control forces of ADSMC (blue line) and AFDSMC (red line), it can be seen that there is no severe chattering phenomenon in control forces. This implies that adding fractional order terms in the sliding surface can also reduce chattering in control forces.

TABLE 1. Parameters in the design of ADSMC and AFDSMC.

Controller parameters	symbol	ADSMC	AFDSMC	AFDSMC	AFDSMC	AFDSMC
sliding surface Parameter 2#	c_2	$\begin{bmatrix}1 & 0\\ 0 & 1\end{bmatrix}$	$\begin{bmatrix}1 & 0\\ 0 & 1\end{bmatrix}$	$\begin{bmatrix}1 & 0\\ 0 & 1\end{bmatrix}$	$\begin{bmatrix}1 & 0\\ 0 & 1\end{bmatrix}$	$\begin{bmatrix}1 & 0\\ 0 & 1\end{bmatrix}$
sliding surface Parameter 3#	c_3	N/A	$\begin{bmatrix}1 & 0\\ 0 & 1\end{bmatrix}$	$\begin{bmatrix}1 & 0\\ 0 & 1\end{bmatrix}$	$\begin{bmatrix}1 & 0\\ 0 & 1\end{bmatrix}$	$\begin{bmatrix}1 & 0\\ 0 & 1\end{bmatrix}$
Fractional order	$\alpha-1$	N/A	0.3	0.85	0.15	1.85
Dynamic sliding surface Parameter	∂	$\begin{bmatrix}1 & 0\\ 0 & 1\end{bmatrix}$	$\begin{bmatrix}1 & 0\\ 0 & 1\end{bmatrix}$	$\begin{bmatrix}1 & 0\\ 0 & 1\end{bmatrix}$	$\begin{bmatrix}1 & 0\\ 0 & 1\end{bmatrix}$	$\begin{bmatrix}1 & 0\\ 0 & 1\end{bmatrix}$
Robust gain	η	$\begin{bmatrix}50 & 0\\ 0 & 50\end{bmatrix}$	$\begin{bmatrix}50 & 0\\ 0 & 50\end{bmatrix}$	$\begin{bmatrix}50 & 0\\ 0 & 50\end{bmatrix}$	$\begin{bmatrix}50 & 0\\ 0 & 50\end{bmatrix}$	$\begin{bmatrix}50 & 0\\ 0 & 50\end{bmatrix}$
Gain of (24)	η_1	10	10	10	10	10
Gain of (25)	η_2	20	20	20	20	20
Gain of (26)	η_3	50	50	50	50	50

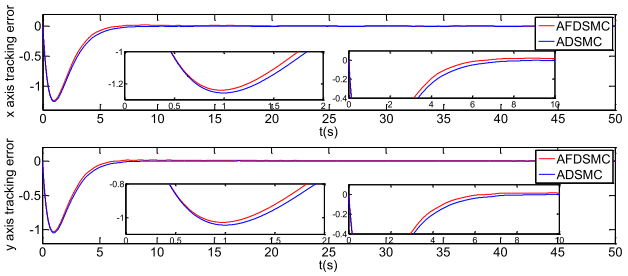

FIGURE 3. Tracking errors using ADSMC and AFDSMC.

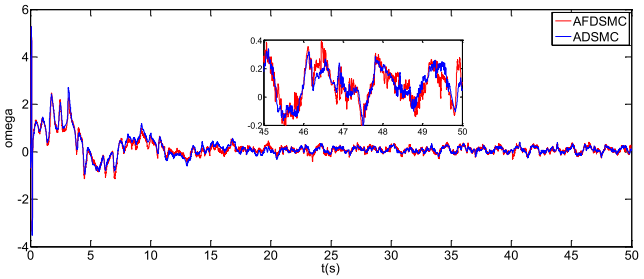

FIGURE 5. Adaptation of angular velocity of ADSMC and AFDSMC.

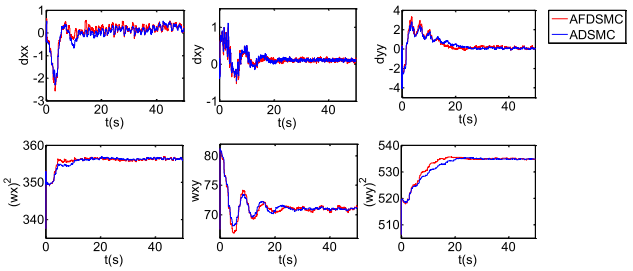

FIGURE 4. Adaptation of parameters of ADSMC and AFDSMC.

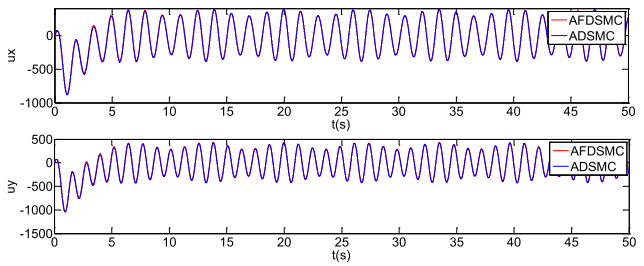

FIGURE 6. Control forces of ADSMC and AFDSMC.

B. SYSTEM DYNAMIC AND PARAMETER ADAPTATION USING AFDSMC UNDER DIFFERENT FRACTIONAL ORDERS

It shall be claimed that all the parameters in all the simulation cases in this part are all the same except the fractional order in the sliding surface. It can be seen from Fig.7-Fig.11 that there are 4 different color lines where green line represents $\alpha-1=0.3$, pink line represents $\alpha-1=0.85$, red line represents $\alpha-1=-0.15$ and blue line represents $\alpha-1=-0.85$. The positive fractional orders represent derivation operation and negative fractional orders represent integration operation.

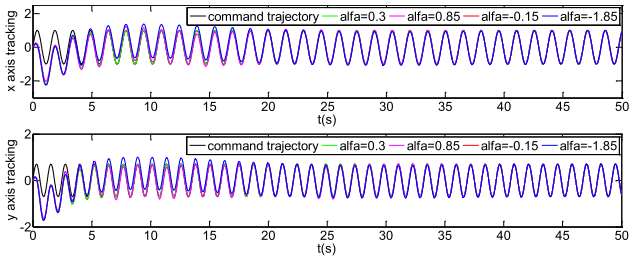

FIGURE 7. Tracking performances of AFDSMC under different factional orders.

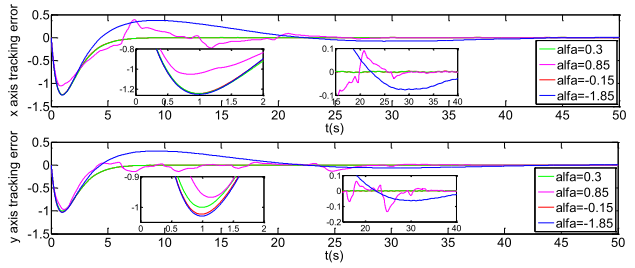

FIGURE 8. Tracking errors of AFDSMC under different factional orders.

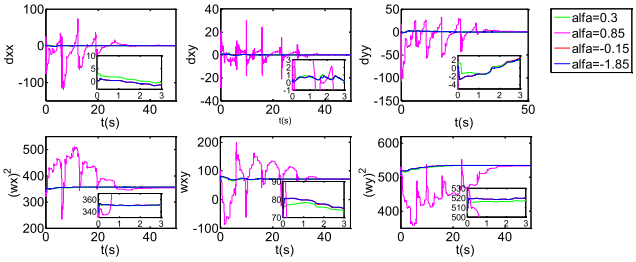

FIGURE 9. Adaptation of parameters using AFDSMC under different factional.

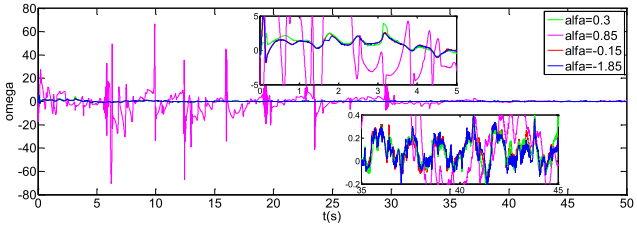

FIGURE 10. Adaptation of angular velocity using AFDSMC under different factional orders.

System dynamics and tracking errors under AFDSMC with different fractional orders are shown in Fig.7 and Fig.8. It can be found from Fig.7 that all the 4 lines can track the black line (command trajectory) in a few seconds and the 4 lines almost overlap with each other in the end. It can be seen from Fig.8 that all the tracking errors under different fractional orders will converge to zero and it can be observed from the partial enlarged pictures in both tracking error figures that pink lines ($\alpha - 1 = 0.85$) have more rapid response than the other 3 lines while green line ($\alpha - 1 = 0.3$) responses more quickly than the other 2. This implies that adding fractional

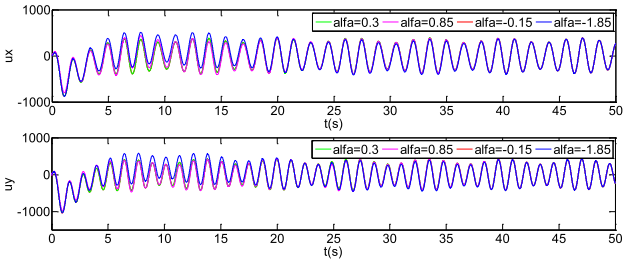

FIGURE 11. Control forces using AFDSMC under different factional orders.

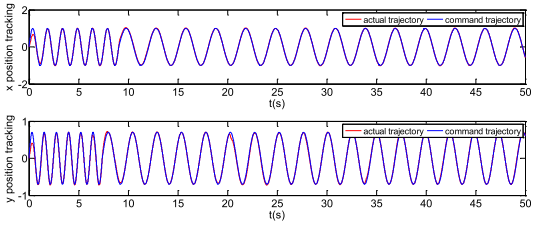

FIGURE 12. Tracking performances of AFDSMC under frequency deviation.

order derivative terms in the sliding surface can accelerate system response, but a too strong derivative order term (pink line $\alpha - 1 = 0.85$) may degrade system tracking performance where some oscillations can be observed in the pink line ($\alpha - 1 = 0.85$). Comparing blue line ($\alpha - 1 = -1.85$) with pink line ($\alpha - 1 = 0.85$),both lines have some oscillations and both lines use more time than green ($\alpha - 1 = 0.3$) and red lines ($\alpha - 1 = -0.15$) to converge to zero. But there are some differences that the error dynamic of blue line ($\alpha - 1 = -1.85$) is very smooth while the error dynamic of pink line ($\alpha - 1 = 0.85$) is very intense. It can be inferred that big fractional derivative order will result intense system response while big fractional integration order can decelerate system responses.

Adaptation performances of system parameters and angular velocity under different fractional orders are shown in Fig.9 and Fig.10 where pink lines response more intensively than the other 3. Observed from the partial enlarged pictures in each figure, the adaptation progress of pink line and green line is more rapid than the other 2. This situation is also in accordance with error dynamics in Fig.8.

Fig.11 depicts control forces under different fractional orders showing that different fractional order terms can adjust system dynamics without causing chattering phenomenon.

C. TRACKING PERFORMANCES EVALUATION UNDER FREQUENCY DEVIATION

Control performances using AFDSMC under different fractional orders have been provided in part 4.1 and 4.2. in order to investigate performances of the control system under frequency deviation, we provide results when frequencies of command signals changes from frequency A to frequency B.

Fig.12 and fig.13 depicts tracking performances and tracking errors under frequency deviation. It can be seen from

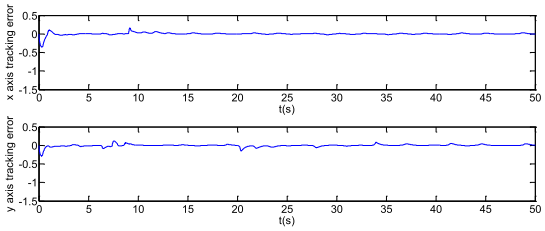

FIGURE 13. Tracking error of AFDSMC under frequency deviation.

tracking performance in fig.12 that frequency of command signal in X and Y axis changes from $x_d = \sin(4.11t)$ to $x_d = \sin(2.085t)$ and $y_d = 0.7\sin(5.11t)$ to $y_d = 0.7\sin(2.555t)$ at time point $t = 12\pi/4.17$ and $t = 12\pi/5.11$ where actual system trajectory can soon track the command trajectory.

V. CONCLUSION

This paper proposes an adaptive fractional order dynamic sliding mode controller for MEMS gyroscopes. Fractional calculus is adopted in the design of dynamic sliding mode control and the new fractional control scheme is applied to a MEMS gyroscope model. Dynamic sliding mode control can help reduce chattering in control forces while fractional calculus can improve system tracking performance. Adaptive control technique is also incorporated in the controller design where the control law and all the adaptive laws are derived in the Lyapunov framework to guarantee the asymptotic stability of the closed-loop system. As long as persistent excitation condition is satisfied, all system parameters including the angular velocity can be correctly estimated. Simulation results verify the validity of the proposed control approach, demonstrating that fractional calculus can improve system tracking performances as well as parameter estimation performance.

ACKNOWLEDGMENT

The authors would like to thank the anonymous reviewers for your useful comments that improved the quality of the article.

REFERENCES

[1] M. Hosseini-Pishrobat and J. Keighobadi, "Robust output regulation of a triaxial MEMS gyroscope via nonlinear active disturbance rejection," *Int. J. Robust Nonlinear Control*, vol. 28, no. 5, pp. 1830–1851, Mar. 2018.
[2] M. Rahmani, "MEMS gyroscope control using a novel compound robust control," *ISA Trans.*, vol. 72, pp. 37–43, Jan. 2017.
[3] R. Park, R. Horowitz, S. K. Hong, and Y. Nam, "Trajectory-switching algorithm for a MEMS gyroscope," *IEEE Trans. Instrum. Meas.*, vol. 56, no. 60, pp. 2561–2569, Dec. 2007.
[4] V. Utkin, "Variable structure systems with sliding modes," *IEEE Trans. Autom. Control*, vol. AC-22, no. 2, pp. 212–222, Apr. 1977.
[5] A. Ferrara, G. P. Incremona, and E. Regolin, "Optimization-based adaptive sliding mode control with application to vehicle dynamics control," *Int. J. Robust Nonlinear Control*, vol. 29, no. 3, pp. 550–564, Feb. 2019.
[6] S. Keshtkar and A. Poznyak, "Tethered space orientation via adaptive sliding mode," *Int. J. Robust Nonlinear Control*, vol. 26, no. 8, pp. 1632–1646, May 2016.
[7] C.-L. Hwang, C.-C. Yang, and J. Y. Hung, "Path tracking of an autonomous ground vehicle with different payloads by hierarchical improved fuzzy dynamic sliding-mode control," *IEEE Trans. Fuzzy Syst.*, vol. 26, no. 2, pp. 899–914, Apr. 2018.
[8] X. Liu, S. Qi, R. Malekain, and Z. Li, "Observer-based composite adaptive dynamic terminal sliding-mode controller for nonlinear uncertain SISO systems," *Int. J. Control, Autom. Syst.*, vol. 17, no. 1, pp. 94–106, Jan. 2019.
[9] V. Utkin, "Discussion aspects of high-order sliding mode control," *IEEE Trans. Autom. Control*, vol. 61, no. 3, pp. 829–833, Mar. 2016.
[10] A. Chalanga, S. Kamal, L. M. Fridman, B. Bandyopadhyay, and J. A. Moreno, "Implementation of super-twisting control: Super-twisting and higher order sliding-mode observer-based approaches," *IEEE Trans. Ind. Electron.*, vol. 63, no. 6, pp. 3677–3685, Jun. 2016.
[11] P. Ioannou and J. Sun, *Robust Adaptive Control*. Upper Saddle River, NJ, USA: Prentice-Hall, 1996.
[12] J. Fei, W. Yan, and Y. Yang, "Adaptive nonsingular terminal sliding mode control of MEMS gyroscope based on backstepping design," *Int. J. Adapt. Control Signal Process.*, vol. 29, no. 9, pp. 1099–1115, Sep. 2015.
[13] C. Lu and J. Fei, "Adaptive prescribed performance sliding mode control of MEMS gyroscope," *Trans. Inst. Meas. Control*, vol. 40, no. 2, pp. 400–412, 2016.
[14] A. Banazadeh and N. Taymourtash, "Adaptive attitude and position control of an insect-like flapping wing air vehicle," *Nonlinear Dyn.*, vol. 85, no. 1, pp. 47–66, Jul. 2016.
[15] Q. Hu, X. Shao, and L. Guo, "Adaptive fault-tolerant attitude tracking control of spacecraft with prescribed performance," *IEEE/ASME Trans. Mechatronics*, vol. 23, no. 1, pp. 331–341, Feb. 2018.
[16] B. Wu, G.-H. Yang, H. Wang, and F. Wang, "Adaptive fuzzy asymptotic tracking control of uncertain nonaffine nonlinear systems with non-symmetric dead-zone nonlinearities," *Inf. Sci.*, vol. 348, pp. 1–14, Jun. 2016.
[17] H. Wang, P. X. Liu, X. Zhao, and X. Liu, "Adaptive fuzzy finite-time control of nonlinear systems with actuator faults," *IEEE Trans. Cybern.*, to be published. doi: 10.1109/TCYB.2019.2902868.
[18] H. Wang, P. X. Liu, X. Xie, and X. Liu, "Adaptive fuzzy asymptotical tracking control of nonlinear systems with unmodeled dynamics and quantized actuator," *Inf. Sci.*, to be published. doi: 10.1016/j.ins.2018.04.011.
[19] Y. Yin, G. Zong, and X. Zhao, "Improved stability criteria for switched positive linear systems with average dwell time switching," *J. Franklin Inst.*, vol. 354, no. 8, pp. 3472–3484, May 2017.
[20] X. Zhao, X. Wang, S. Zhang, and G. Zong, "Adaptive neural backstepping control design for a class of nonsmooth nonlinear systems," *IEEE Trans. Syst., Man, Cybern. Syst.*, vol. 49, no. 9, pp. 1820–1831, Sep. 2019. doi: 10.1109/tsmc.2018.2875947.
[21] J. Fei and C. Lu, "Adaptive fractional order sliding mode controller with neural estimator," *J. Franklin Inst.*, vol. 355, no. 5, pp. 2369–2391, 2018.
[22] A. Hajipour and H. Tavakoli, "Dynamic analysis and adaptive sliding mode controller for a chaotic fractional incommensurate order financial system," *Int. J. Bifurcation Chaos*, vol. 27, no. 13, Dec. 2017, Art. no. 1750198.
[23] A. Karami-Mollaee, H. Tirandaz, and O. Barambones, "On dynamic sliding mode control of nonlinear fractional-order systems using sliding observer," *Nonlinear Dyn.*, vol. 92, no. 3, pp. 1379–1393, May 2018.
[24] K. Oldham and J. Spanier, *The Fractional Calculus*. New York, NY, USA: Academic, 1974.
[25] I. Podlubny, *Fractional Differential Equations*. San Diego, CA, USA: Academic, 1999.
[26] Y. Q. Chen and K. L. Moore, "Discretization schemes for fractional-order differentiators and integrators," *IEEE Trans. Circuits Syst. I, Fundam. Theory Appl.*, vol. 49, no. 3, pp. 363–367, Mar. 2002.
[27] A. Oustaloup, B. Mathieu, and P. Lanusse, "The CRONE control of resonant plants: Application to a flexible transmission," *Eur. J. Control*, vol. 1, no. 2, pp. 113–121, 1995.